Channeling Acceleration in Crystals and Nanostructures and Studies of Solid Plasmas: New Opportunities

Robert Ariniello[1], Sebastien Corde[2], Xavier Davoine[3], Henrik Ekerfelt[4], Frederico Fiuza[4], Max Gilljohann[2], Laurent Gremillet[3], Yuliia Mankovska[2], Henryk Piekarz[5], Pablo San Miguel Claveria[2], Vladimir Shiltsev[5], Peter Taborek[6], and Toshiki Tajima[6]

[1]University of Colorado Boulder, Boulder, CO 80309, USA
[2]Ecole Polytechnique, 91128 Palaiseau, France
[3]CEA, DAM, DIF, F-91297 Arpajon, France
[4]SLAC National Accelerator Laboratory, Stanford, CA 94025m, USA
[5]Fermilab, Batavia, IL 60510, USA
[6]University of California Irvine, Irvine, CA 92697, USA ,

March 16, 2022

1 Executive Summary

Plasma wakefield acceleration (PWA) has shown illustrious progress over the past two decades of active research and resulted in an impressive demonstration of $O(10 \text{ GeV})$ particle acceleration in $O(1 \text{ m})$ long single structures. While already potentially sufficient for some applications, like, e.g., FELs, the traditional laser- and beam-driven acceleration in gaseous plasma faces enormous challenges when it comes to the design of the PWA-based $O(1\text{-}10 \text{ TeV})$ high energy e^+e^- colliders due to the complexity of energy staging, low average geometric gradients, and unprecedented transverse and longitudinal stability requirements. **Channeling acceleration in solid-state plasma of crystals or nanostructures, e.g., carbon nanotubes (CNTs) or alumna honeycomb holes, has the promise of ultra-high accelerating gradients $O(1\text{-}10 \text{ TeV/m})$, continuous focusing of channeling particles without need of staging, and ultimately small equilibrium beam emittances naturally obtained while accelerating.**

Several methods of wakefield excitation are being considered including ultra-short or micro-bunched electron beams and laser pulses, ion clusters, etc. While beams of muons are the most suitable for potential future high energy physics colliders based on the crystal-PWA, most of the proof-of-principle demonstrations can be carried out with electrons at the leading existing and planned accelerator and/or laser research facilities, such as FACET-II, ELI, and others. **We call for support of these experimental efforts augmented with corresponding PIC plasma simulation and actively seek new collaborators to carry out and expand the ongoing R&D program. We consider demonstration by the end of this decade of 1 GeV acceleration over 1 mm of solid crystal/CNT structure as a viable goal**.

Recently started E336 collaboration will study excitation of transverse and longitudinal wakefields by an ultra-dense FACET-II electron bunch in evacuated channels such as stacks of CNTs or micron- or submicron channel arrays in $O(1 \text{ mm})$ long dielectric targets. PIC simulations indicate that even with the micron-scale FACET-II bunches that extend over many nano- or micro-tubes, the PWA effects will result in beam nanomodulation and an easily detectable expansion of the angular spread of the 10-GeV beam electrons, far exceeding that from just a multiple scattering process. Next phase of the E336 experiments will study formation of the beam nano-bunches in the solid plasma, observation of the betatron radiation, and, eventually, particle acceleration by ultra-strong longitudinal wakefields.

Required also is an in-depth research on dynamics of *beam-plasma instabilities* in ultra-dense plasma, its development and suppression in structured media like CNTs and crystals, and its potential use as a pre-modulator or as an amplifier for easier detection of the imprint of the nanostructure on the beam in E336 experiment. The recent invention of the *thin film compression* technique opens the way to introduce the availability of the single-cycled laser pulse and thus the relativistic compressed X-ray laser pulse, which fits the need for X-ray-driven nanostructure PWA. Given the tremendous promise of the crystal/CNT channeling acceleration and the not-yet fully explored complexity of the beam, laser and plasma physics involved in corresponding phenomena at the nanometer scales, exploration of promising near-term applications, serious theoretical analysis, and advanced computer

modeling efforts are essential to make the concept sufficiently investigated and its feasibility for future colliders established.

2   Introduction: Wakefield Acceleration in Solid Nano-structures

The feasibility of the future colliders critically depends on their energy reach, luminosity, cost, length, and power efficiency [1]. So far, the most advanced of the proposals for the energy frontier colliders call for acceleration by wakefields in plasma which can be excited by: lasers (demonstrated electron energy gain of about 8 GeV over 20 cm of plasma with density $3 \cdot 10^{17} \mathrm{cm}^{-3}$ at the BELLA facility at LBNL); very short electron bunches (9 GeV gain over 1.3m of $\sim 10^{17} \mathrm{cm}^{-3}$ plasma at FACET facility in SLAC) and by proton bunches (some 2 GeV gain over 10 m of $10^{15} \mathrm{cm}^{-3}$ plasma at the AWAKE experiment at CERN). In principle, the plasma wakefield acceleration (PWA) is thought to make possible multi-TeV e+e- colliders. There is a number of critical issues to resolve along that path, though, such as the power efficiency of the laser/beam PWFA schemes; acceleration of positrons (which are defocused when accelerated in plasma); efficiency of staging (beam transfer and matching from one short plasma accelerator cell to another); beam emittance control in scattering media; and beamstrahlung (radiation due to beam-beam interaction) that leads to the rms energy spread at IP of about 30% for 10 TeV machines and 80% for a 30 TeV collider.

Assessments of options for "ultimate" future energy frontier collider facility with c.o.m. energies far beyond 14 TeV LHC (most powerful modern accelerators) shows [1, 2] that for the same reason the circular e+e- collider energies do not extend beyond the Higgs factory range (0.25 TeV), there will be no circular proton-proton colliders beyond 100 TeV because of unacceptable synchrotron radiation power – therefore, the colliders will have to be linear. Moreover, electrons and positrons even in linear accelerators become impractical above about 3 TeV due to growing facility site power demands, beamstrahlung at the IPs, and, if beyond about 10 TeV, due to the radiation in the focusing channel. If one goes further and requests such a flagship machine not to exceed 10 km in length then an accelerator technology is needed to provide an average accelerating gradient of over 30 GeV/m (to be compared with equivalent ∼0.5 GeV per meter in the LHC). There is only one such option known now: super-dense plasma as, e.g., in crystals [3], which excludes protons because of nuclear interactions and leaves us with muons as the particles of choice. Indeed, the density of charge carriers (conduction electrons) in solids $n_0 \sim 10^{22-24} \mathrm{cm}^{-3}$ is significantly higher than that in gaseous plasma, and correspondingly, the longitudinal accelerating fields of up to 100-1000 GeV/cm (10-100 TV/m) are possible according to

$$E[\mathrm{GV/m}] = m_e \omega_p c/e \approx 100 \sqrt{n_0 [10^{18} \mathrm{cm}^{-3}]}. \tag{1}$$

Acceleration of muons (instead of electrons or hadrons) in crystals or carbon nanotubes with charge carrier density $10^{22-23} \mathrm{cm}^{-3}$ has the promise of the maximum theoretical accelerating gradients of 1-10 TeV/m allowing to envision a compact 1 PeV linear crystal muon collider [4]. High luminosity can not be expected for such a facility if the beam power P is

limited at, e.g., $P \leq 100$MW. In that case, the beam current will have to go down with the particle energy as $I = P/E$, and, consequently, the luminosity will by necessity to go down with energy E, the trend that can be only partially reset by formation of ultra-small $O(1$ A) beam sizes at the collision points.

Ultimate fast 1-10 TeV/m PWA of muons (instead of electrons or hadrons) channeling between the planes in crystals or inside carbon nanostructures (CNT) allows a compact $O(1$ PeV) linear crystal muon collider. The choice of muons is beneficial because of small scattering on solid media electrons, absence of beamstrahlung effects at the IP, and continuous focusing while channeling in crystals, i.e., acceleration to final energy can be done in a single stage. Muon decay becomes practically irrelevant in such very fast acceleration gradients as muon lifetime quickly grows with energy as $2.2\mu s \times \gamma$. Initial luminosity analysis of such machines assumes a small number of muons per bunch $O(1000)$, a small number of bunches $O(100)$, high repetition rate $O(1$ MHz) and ultimately small sizes and overlap of the colliding beams $O(1$ A) - see Sec. 5 below. In general, excitation of wakefields in crystals or nanostructures can be possible by either short sub-μm high-density bunches of X-ray laser pulses (mentioned earlier) or charged particles by electrons, high-Z ions, or by premodulated or self-modulated very high current bunches - see Fig. 1. For example, bunches of charged particles can excite plasma effectively if their transverse and longitudinal sizes are comparable or shorter than the plasma wavelength $\lambda_p \sim 0.3$ μm for $n_0 = 10^{22}$ cm^{-3} and the total number of particles in that volume approaches the number of free electrons in the solid plasma $\sim n_0 \lambda_p^3$.
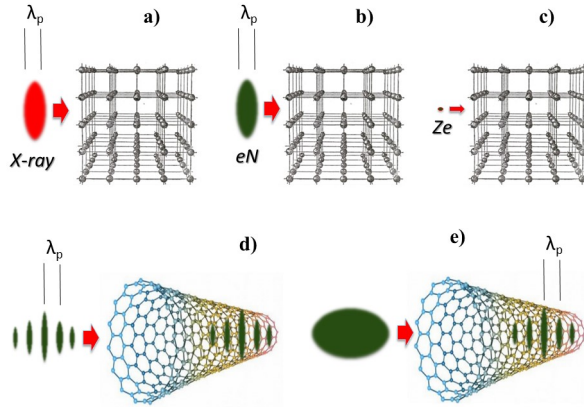

Figure 1: Possible ways to excite plasma wakefields in crystals or/and nanostructures: a) by short X-ray laser pulses; b) by short high density bunches of charged particles; c) by heavy high-Z ions; d) by modulated high current beams; e) by longer bunches experiencing self modulation instability in the media.

There are several critical phenomena in the solid plasma due to intense energy radiation in high fields and increased scattering rates which result in fast pitch-angle diffusion over distances of $l[m] \simeq E[\text{TeV}]$. The scatter leads to particles escaping from the driving field;

thus, it was suggested that particles (muons) to be accelerated in solids along with major crystallographic directions, which provide a channeling effect in combination with low emittance determined by an Angstrom-scale aperture of the atomic tubes [5, 6]. Channeling in the nanotubes was later brought up as a promising option [7, 8, 9, 10]. Positively charged particles are channeled more robustly, as they get repelled from ions and, thus, experience weaker scattering. Radiation emission due to the betatron oscillations between the atomic planes is thought to be the major source of energy dissipation, and the maximum beam energies are limited to about 0.3 TeV for positrons, 10 PeV for muons and 1000 PeV for protons [5]. For energies of 1 to 10 PeV, muons offer much more attraction because they are point-like elementary particles and, contrary to protons, do not carry an intrinsic energy spread of elementary constituents; and they can much easier propagate in solid plasma than protons which will extinct due to nuclear interactions. Very high gradient crystal/CNT accelerators might need to be disposable if the externally excited fields exceed the ionization thresholds and destroy the periodic atomic structure of the crystal (so acceleration will take place only in a short time before full dissociation of the lattice). For the fields of about 1 GV/cm=0.1 TV/m or less, reusable crystal accelerators can probably be built which can survive multiple pulses.

3   Wakefields in Solid Media (Amorphous and Structured)

The introduction of crystals and nanotubes into compact accelerators has been motivated by several directions. One was induced by the potential emergence of a new X-ray laser technology [11] that allows the optical laser tuning into an X-ray laser, thus the operating regime of laser-driven wakefields entering much higher density than gas [12]. It is also driven by the progress in obtaining far shorter and more dense of electron-bunches than with the previously available techniques, exemplified by the SLAC FACET-II facility [13]. Such ultra-short electron bunches can now interact with much higher density medium such as nanotubes [14] (or even solids). The flexibility to choose the average electron density of nanotubes also introduces a possibility to adjust resonant wakefield excitation at various pulse length, dielectric variabilities, and geometry that may be controlled by emerging nanotechnology. For example, hollow nanomaterials may be manufacturable. Possibility to control such materials to the level beyond what is possible for gaseous plasma is one of the potential advantages of using the nanotubes. The nanotubes (or its flat version, graphene) have electrical conductivity on the plane of the graphene greater than that of silver. This arises due to the quantum mechanical benzene electronic property. On the other hand, the electrons are covalently tied to the graphene plane in the direction perpendicular to the graphene plane. Thus electrons can move freely along the graphene plane if the ponderomotive force is in that direction and the wakefield causing electrostatic force is also in that direction. This is a very useful property of nanotubes.

Ref. [8] examined the effects of hollow nanotube structure vs. uniform nanomaterials for X-ray-driven laser wakefield acceleration. Figure 2 compares the wakefield intensity, its shape and stability, the electron dynamics by these wakefields. With the hollow nanostructure, the electron acceleration and dynamics are found to be superior. Also, it is evident
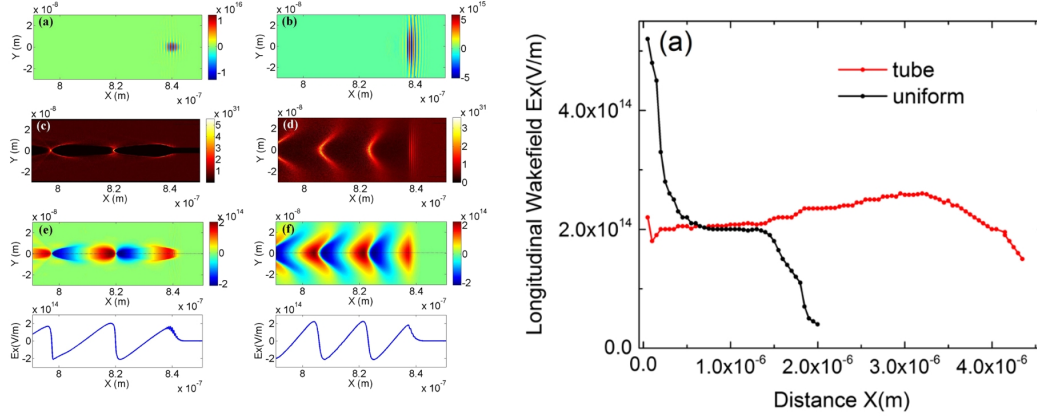
Figure 2: Left - Wakefield excitation in a tube by X-ray laser pulse (left colum of plots) in comparison with a wakefield in a uniform system (right column). Shown are distributions of the laser field - (a) and (b), electron density- (c) and (d), and (e) and (f) longitudinal wakefield - (e) and (f). X-ray pulse spot size of 5 nm and length of 3 nm. Right - in the case of amorphous media the laser field (and wakefields) decreases rapidly with the propagation distance. In the nanotube, the X-ray pulse maintains a small spot size and propagates over much longer distance generating strong nonlinear wakefields (from Ref. [8]).

that the accelerating gradients are ultra-high, as expected due to correspondingly higher electron density of the materials that supports the wakefield - per Eq.(1). Figure 3 presents scaling of the wakefields in simulations which are found close to those predicated by theory. Previous simulation studies of wakefields driven by short electron bunches [15] indicate similar behavior as that reported in [8]. In addition, one can be interested in the properties of nanotubes (and nanomaterials) due to their ionic structures studied in [16]. The wakefield properties are found to be generally similar even if the optical phonon effects due to the lattice structure are incorporated [17].
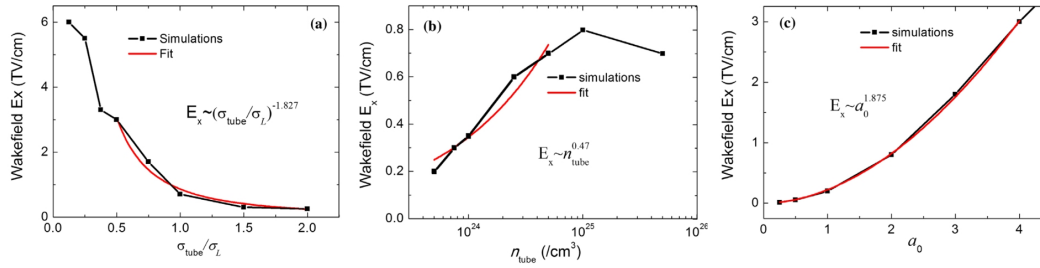

Figure 3: Scaling of the wakefield excited by X-ray pulse: (a) with the tube radius, (b) with the tube wall density if the tube radius fixed $\sigma_{tube} = \sigma_L$, and (c) with laser intensity when the tube radius is $\sigma_{tube} = \sigma_L/2$ (from Ref. [8]).

4 Prospective Experimental Studies

4.1 Near-term prospect for beam solid-plasma experiments

Although the ultimate conditions to drive wakefields in nanostructures or crystals require transverse and longitudinal sizes comparable or smaller than the plasma wavelength λ_p, which ranges from 30 to 300 nm for densities n_p from $1 \times 10^{24}\,\mathrm{cm}^{-3}$ to $1 \times 10^{22}\,\mathrm{cm}^{-3}$, first experimental tests can be carried out before these conditions are reached. This is the purpose of the E-336 experiment that is planned to be conducted with the FACET-II accelerator facility [13] at SLAC National Accelerator Laboratory, where the driver is an electron beam whose transverse and longitudinal sizes is expected to be in the range from 1 to 10μ m. Together with its $2\,\mathrm{nC}$ charge, $10\,\mathrm{GeV}$ beam energy and low emittance of $\sim$10 mm mrad, such beam is relevant to understand the physics developing at the scale of λ_p when the electron beam propagates and interacts with a solid media that is either amorphous (E-305 experiment) and nanostructured (E-336 experiment).

In an amorphous solid, because both longitudinal and transverse sizes are large compared to λ_p, wakefield excitation is very inefficient, and in addition wakefields can be damped by collisional effects. What is left to the plasma response is the return current that flows through the beam, and leads to an unstable counterstreaming system of beam and plasma electrons, where any perturbation at the scale of λ_p can grow exponentially as the beam propagates through the solid. For an ultrarelativistic beam such as the one delivered by FACET-II, two modes of instability are prominent: the oblique two-stream instability (OTSI) [18], which is mainly electrostatic and with a wave vector at an oblique angle with respect to the beam propagation, and the current filamentation instability (CFI),
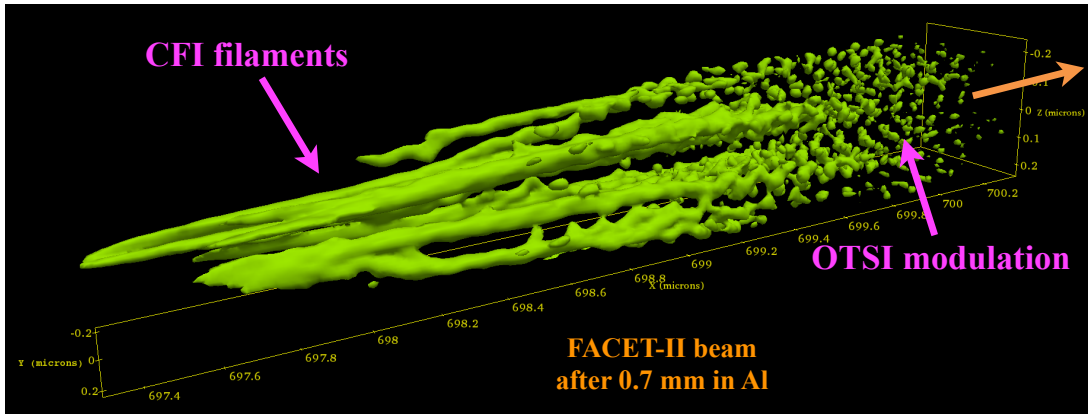

Figure 4: 3D PIC simulation of the 10 GeV FACET-II electron beam interacting with an Al solid target. After 0.7 mm of propagation, strong oblique modulations (OTSI) have built up at the beam front (right), which evolve into transverse filaments (CFI) when moving toward the rear of the beam (left). The simulation was run using the CALDER 3D PIC code [19], with a peak beam density $n_b = 1 \times 10^{20}\,\mathrm{cm}^{-3}$, a normalized transverse emittance of $3\,\mathrm{mm}\,\mathrm{mrad}$, a bunch length of 1μ m and with periodic boundary conditions in the transverse directions.

which is mainly magnetic and transverse. This is exemplified in Fig. 4 showing the FACET-II electron beam after 0.7 mm of propagation through aluminum, as simulated using the CALDER 3D PIC code [19]. At the front of the beam (right of Fig. 4), longitudinal and transverse modulations are clearly observed and correspond to the OTSI instability, which is the fastest mode to grow in the linear phase [18]. In contrast, at the rear of the beam, beam filaments can be identified and attributed to the CFI instability. The interplay between these two modes that appear respectively at the beam front and rear of the beam can be understood by the variation of the collisionality as the plasma electrons are heated when flowing from the front to the rear of the beam. In this CALDER simulation and with the considered beam and plasma parameters, the higher collisionality at the rear damps the OTSI and favor the CFI instability, thus resulting in the beam profile of Fig. 4). Beyond this imprint that the beam-solid interaction has left on the beam at the scale of λ_p, high-energy beam electrons also experience the very large electromagnetic fields associated with the instability and thus can radiate gamma rays very efficiently [20], and such gamma-ray flashes can also be an excellent experimental observable to diagnose the beam-solid interaction and the physics developing at the scale of λ_p.

In a nanostructured solid, the beam evolution is no longer dictated by the amplification of initial noise perturbation that can exist at the scale of λ_p, but by the imposed structure of the solid. Notably, the beam being much larger than λ_p and than the structure length scale (e.g. the tube diameter), it fills both the vacuum and solid parts of the structure, and many periods transversely (see Fig. 5). While the beam self fields can exist in the vacuum tubes of the nanostructure, they are shielded in the solid which results in the excitation of wakefields and to the channeling of beam electrons in the vacuum tubes. The physics also differ depending on the typical length scale of the structure. For a tube diameter much larger than λ_p, shielding is done over a skin depth that is much smaller than the tube diameter and thus the solid plasma response is mainly driven on the tube surface. In contrast to this surface response, for tube diameter of the order of λ_p or smaller, the response of plasma electrons can become more volumetric.

A typical outcome of beam-nanotarget interaction is depicted in Fig. 5, for a beam whose size and length is very large compared to the nanostructure period and to λ_p. The density of the 10 GeV beam after mm-scale propagation (see middle row of Fig. 5) clearly exhibits nanomodulation at the nanostructure period, with maximums located in the vacuum gaps. The transverse phase space of the beam (see bottom of Fig. 5) shows that the transverse momentum spread, and thus the angular spread, is greatly increased due to the beam-nanotarget interaction, and it takes the typical shape (see bottom right of Fig. 5) associated to trapped beam electron orbits (around the peaks visible in the phase space). This demonstrates the channeling principle with beam electrons being captured and trapped in the vacuum gaps. Beyond nanomodulations and growth of angular spread, an additional experimental observable is the generation of radiation, similarly to the case of amorphous solid. Indeed, the channeling of beam electrons in the vacuum tubes leads to the emission of betatron-like radiation by beam electrons oscillating about the axis of the tube, radiation whose frequency can provide a direct measurement of the particle oscillation period and thus of the focusing force in the tube.
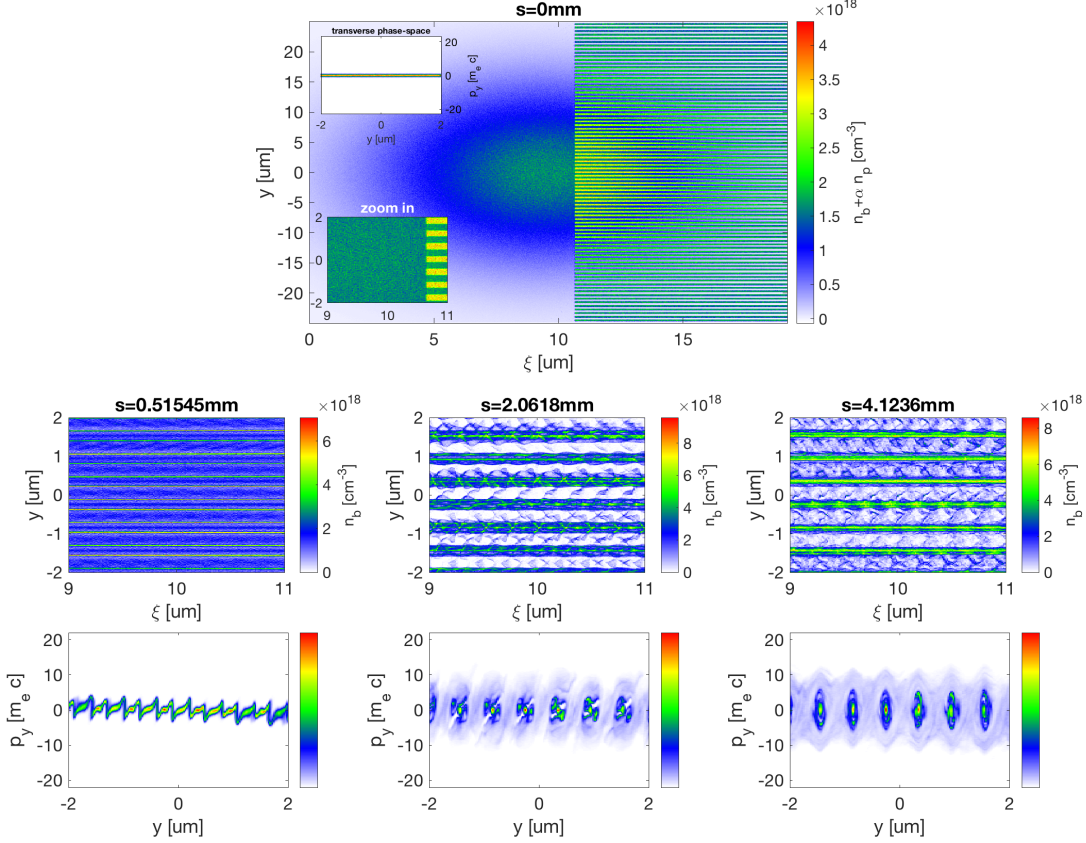
Figure 5: 2D PIC simulation of the 10 GeV FACET-II electron beam interacting with a nanostructured target. The target (see top figure) consists in 300-nm-wide vacuum gaps separated by 300-nm-wide plasma sections of electron density $n_p = 2 \times 10^{22} \, \mathrm{cm^{-3}}$. The beam density (middle row) and transverse phase space (bottom row) are shown after different propagation distances ($s = 0.5, 2.1, 4.1 \, \mathrm{mm}$). The simulation was run using the CALDER 2D PIC code [19], with a beam charge of 2 nC, a peak current of 50 kA, a normalized transverse emittance of 5 mm mrad and a beam size of 10μ m.

Another new opportunity opened by the study of the response of solid plasmas to extreme beams is to take advantage of both amorphous and nanostructured solids. An interesting geometry is to start by a nanostructured target, that can be understood as a pre-modulator for the beam, and then go into an amorphous solid that can work as an amplifier where the instability will take place and will leave a strong imprint on the beam and on the level of gamma-ray emission. Such scenario is of interest first because the nanotarget induces a nanomodulation that acts as a seed for the instability in the amorphous solid, but also because the experimental observation of the instability after the nanotarget can reveal very effectively that a process of nanomodulation indeed took place in the nanotarget. This strategy thus allows us to be extremely sensitive to the beam evolution in the nanotarget. The principle is illustrated in Fig. 6 by a CALDER 2D PIC simulation. In conditions for which no instability is observed when only the uniform plasma is present (see right column
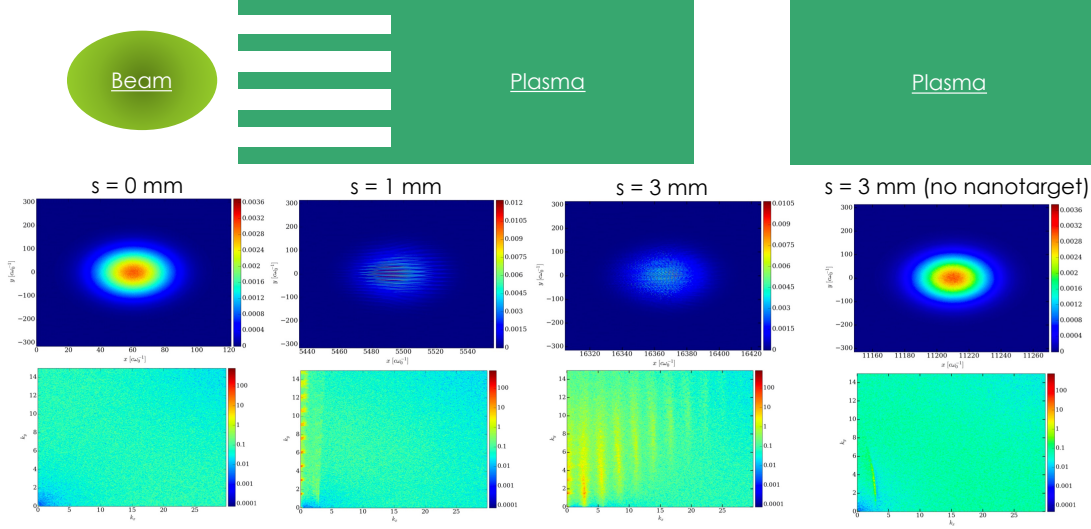
9

Figure 6: 2D PIC simulation of the 10 GeV FACET-II electron beam interacting with a 1-mm-long nanostructured target followed by a 2-mm-long uniform plasma (see top left). The beam density (middle row) and its Fourier transform (bottom row) are shown after different propagation distances corresponding to the start of the simulation ($s = 0\,\mathrm{mm}$), the end of the nanotarget ($s = 1\,\mathrm{mm}$) and the end of the uniform plasma ($s = 3\,\mathrm{mm}$), as well as for the case without nanotarget (right column, 2-mm-long uniform plasma only).

of Fig. 6), the addition of a 1-mm-long nanostructured target induces a purely transverse modulation in the beam density with peaks appearing only at $k_\parallel = 0$ in its Fourier transform and corresponding to the harmonics of the spatial frequency of the nanostructure (see second column corresponding to $s = 1\,\mathrm{mm}$ in Fig. 6). After going through the 2-mm-long uniform plasma, the pre-modulation from the nanotarget allows the beam to undergo the instability with a very strong longitudinal modulation characteristic of the OTSI (with peaks in the Fourier transform when $k_\parallel$ is a multiple of k_p) and a transverse modulation that spans $k_\perp$ continuously in the Fourier transform (instead of being multiple of the nanostructure spatial frequency). Because this strong instability-driven beam modulation (see bottom row and third column of Fig. 6) is only present when there is a nanostructured target to pre-modulate the beam, this simulation result illustrates how this scheme can provide an experimental signature that is very sensitive to the nanomodulation from the nanostructured target. For instance, transition radiation emitted as the beam exits the uniform plasma will exhibit the longitudinal structure of the beam, and its spectrum will thus reveal the longitudinal beam modulation that is reminiscent of the nanomodulation from the nanostructured target.

4.2   Paths and facilities for follow-up experiments

To go beyond these near-term experiments, novel developments and facilities are required. Indeed, ultimately we need drivers (X-ray pulses, electrons or high-Z ions) with transverse

and longitudinal sizes comparable or shorter than the plasma wavelength λ_p at solid density, that is of the order of 0.1μ m. A first objective should be to develop a new capability in accelerator facilities such as FACET-II, that is to deliver electron beams focused transversely to sub-μm beam size, which first require very low emittance beams. Then, thin plasma lenses are excellent candidates to readily focus a beam that is initially few μm in size down to sub-μm sizes, and they open a promising path to reach beam sizes of the order of 0.1μ m, that are relevant for crystal/nanostruture wakefield acceleration. The successuful implementation of such thin plasma lenses in an accelerator facility will thus be a great asset to study wakefield excitation in crystals and nanostructures. Such highly-focused beams could also come from novel high-brightness beam sources such as the plasma photocathode [21], or laser-based schemes by leveraging the capabilities of ultrahigh-power laser systems. The latter can not only provide new sources of electron beams, but also of coherent X-ray pulses.

With this prospective availability of **highly-focused drivers**, one can envision to study crystal/nanostructure wakefield with "long" drivers, that are much longer than λ_p. This can first be achieved by relying on self modulation due to the wakefield in the nanostructure, this modulation being reminiscent of wakefield excitation and thus providing an experimental observable for it, in a way similar to proton bunch self modulation observed in the AWAKE experiment [22, 23]. One can also decouple the process of beam modulation and the excitation of wakefield in the nanostructure by sending a pre-modulated driver into the structure. This could be achieved for instance through self modulation of the beam in an amorphous solid that is preceding the nanostructure. Such advanced experiments will beneficiate from the input of near-term experiments such as E336 at FACET-II, that will provide valuable experimental measurements allowing us to benchmark our theoretical modeling of beam-nanostructure interaction against experimental data. Advanced nanostructure experiments with highly-focused drivers are expected to provide a unique insight into the interaction of ultrahigh-density drivers (in particular electron beams) with crystals and different types of nanostructures such as CNTs and porous alumina or glass nanostructures, and on the resulting incoherent channeling radiation. It will further give valuable experimental data on controlled focusing and self-bunching/slicing/modulation of ultrahigh-density beams in CNTs/crystals, and on the generation and detection of high-amplitude wakefields through the coherent buildup from a pre-modulated beam.

The most challenging development is arguably to deliver **highly-compressed drivers**, first at sub-μm bunch length and ultimately reaching bunch length of the order of 0.1μm. While accelerator facilities such as FACET-II may be able to deliver $\sim \mu$m bunch length with peak current from 100 to 300 kA [13], the experimental demonstration of a 0.1μ m bunch length requires novel developments. This could be done directly through some specific plasma-based and/or laser-based injection schemes, or by re-compressing beams produced in plasma and/or laser wakefield accelerators. Although the characterization of the longitudinal phase space of electron beams from plasma accelerators is still in its infancy, theoretical and numerical modeling suggests that the longitudinal beam quality (in particular the longitudinal emittance) is excellent and the energy spread is actually dominated by correlerated energy spread. Manipulating the longitudinal phase space and re-compressing electron beams from plasma accelerators is thus a very promising approach to reach 0.1μm bunch length with mega-ampere peak currents. For X-ray drivers, the recent invention of the

thin film compression technique promises to deliver relativistically compressed X-ray laser pulses, suited for crystal/nanostructure channeling acceleration. The combined availability of **highly-focused and highly-compressed drivers** will mark a critical milestone, allowing to push considerably the research on crystal/nanostructure wakefield acceleration with its full capability unravelled, that is with the generation of extreme-gradient (TeV/m) wakefields and possibly to coherent sources of X rays and gamma rays. We should emphasize that such an incredible development with extreme highly-focused and highly-compressed drivers will benefiate to the physics community well beyond crystal/nanostructure wakefield acceleration, for example it will be a critical stepping stone on the way to a fully non-perturbative QED collider [24] and will be instrumental to novel schemes that could allow for extremely dense gamma-ray and e^+e^- pair jets and laserless study of strong-field QED [25], both of great interest for our fundamental understanding of the laws of nature and for astrophysics.

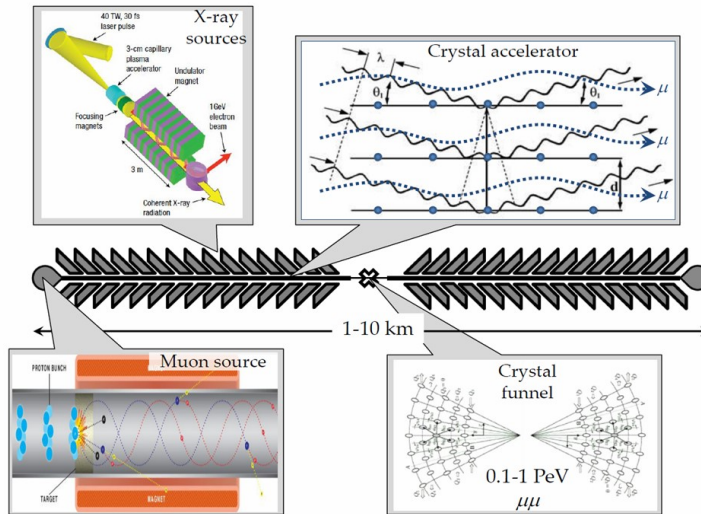# 5 Crystal Channeling Muon Linear Collider Design Principles

Figure 7: Concept of a linear X-ray crystal muon collider (adapted from [4]).

Possible conceptual scheme of a crystal linear muon collider - see Fig. 1 - includes two high brightness muon sources, two continuous crystal linacs of a total length of 1 to 10 km driven by numerous X-ray sources (or other type of drivers) to reach 1-10 PeV c.m.e. at the interaction point with a crystal funnel [4]. Initial luminosity analysis of such machine assumes the minimal overlap area of the colliding beams to the crystal lattice cell size $A \sim 1$ $\mathring{A}^2 = 10^{-16} \mathrm{cm}^{-2}$ and that the crystals in each collider arm are aligned channel to channel. The number of muons per bunch N also can not be made arbitrary high due to the beam loading

effect and should be $N \sim 10^3$. Excitation many parallel atomic channels n_{ch} can increase the luminosity $L = f n_{ch} \ N^2 / A = f \cdot 10^{16} \cdot 10^6 \cdot n_{ch} [\text{cm}^{-2}\text{s}^{-1}]$ which can reach $10^{30} \text{cm}^{-2}\text{s}^{-1}$ at, e.g., $f = 10^6$ Hz and $n_{ch} \sim 100$. Exceeding the value of the product $f n_{ch}$ beyond 10^8 Hz can be very costly as the total beam power $P = f n_{ch} N E_p$ will get beyond a practical limit of ~ 10 MW. Instead, using some kind of *crystal funnel* to bring microbeams from many channels into one can increase the luminosity by a factor of n_{ch} to some $10^{32} \text{cm}^{-2}\text{s}^{-1}$.

6 Application of Crystal/CNT Acceleration

One of the very near term applications of laser wakefield accelerators (LWFA) may be a medical application in the radiation oncology treatment. Unlike the high energy applications of LWFA and beam-driven wakefield accelerators, these medical radiotherapy applications look at the non-relativistic regime of the laser (the normalized laser strength parameter $a_0 ¡ 1$). Some of the researchers in medical radiation oncologists called for a departure from the traditional radiation therapy of cancer and even COVID such as Brachy therapy, due to the safety, convenience, and more accurate targeting of radiation [26, 27, 28]. In low energy electron therapy (such as 10's keV) in some of these therapies (including the surface skin tumor treatments) the electron acceleration is very local using non-relativistic laser intensity [26]. In such non-relativistic electron beam generation, the laser may be operating in $a_0 \ll 1$. Also it may be operated via using a fiber laser. If so, such a fiber laser may be a part of the endoscope that can be inserted into a patient via a medical fiber scope and at its tip the laser may be delivered to a nanofiber target. If so, such a nanofiber targetry driven by laser fiber need not require vacuum nor some other heavy installation and can be handy via an endoscope. We have studied the LWFA operation regime of this and find that there is a great operational latitutde for such a device utilizing the fiber laser, nanotube materials as its target in the non-relativistic regime [26]. This operation is relatively simple and some preliminary experimental pursuits are beginning.

Furthermore, our recent advancement in the vector medicine that seek specific molecules such as cancer cells [29] may be adopted for a further preferred deposition of electron radiation focused onto tumor tissues. In this electron case, as such a vector medicine can be loaded with a high Z-metal, such vector molecules that seek and are attached to the cancer cells can absorb electrons preferentially, as the electron mean-free-path is much shorter for the high-Z matter. It would be of interest to see these predicted behaviors in the low intensity high density LWFA operation.

Another interesting opportunity is possibility to use plasma wakefield acceleration in crystals for generation, capture and fast acceleration of ultra low-emittance, high-energy muon beams, as proposed in Ref.[30].

References

[1] V. Shiltsev and F. Zimmermann, Modern and future colliders *Rev. Mod. Phys.* **93**, 015006 (2021)

[2] V.Shiltsev, General approach to physics limits of ultimate colliders, *Proc. IPAC'21 (May 24-May 28, 2021)* WEPAB017; also FERMILAB-CONF-21-257 (2021).

[3] T.Tajima, M.Cavenago, Crystal X-ray accelerator, *Phys. Rev. Lett.*, **59(13)**, 1440 (1987).

[4] V.Shiltsev, High-energy particle colliders: past 20 years, next 20 years, and beyond, *Physics-Uspekhi* **55, (10)**, 965 (2012).

[5] P.Chen, R.Noble, Crystal channel collider: ultra-high energy and luminosity in the next century, in *AIP Conference Proceedings* **398(1)**, 273 (1997).

[6] I.Dodin, N.Fisch, Charged particle acceleration in dense plasma channels, *Phys. Plasmas* **15(10)**, 103105 (2008).

[7] T.Tajima, *et al.,* Beam transport in the crystal X-ray accelerator, *Part. Accel.* **32** 235 (1989).

[8] X.Zhang, *et al.,* Particle-in-cell simulation of X-ray wakefield acceleration and betatron radiation in nanotubes, *Phys. Rev. Accel. Beams* **19(10)** 101004 (2016).

[9] Y.M.Shin, D.Still, V.Shiltsev, X-ray driven channeling acceleration in crystals and carbon nanotubes, *Phys. Plasmas* **20(12)**, 123106 (2013).

[10] Y.M.Shin, A.Lumpkin, R.Thurman-Keup. TeV/m nano-accelerator: Investigation on feasibility of CNT-channeling acceleration at Fermilab, *Nucl. Instr. Meth. B* **355**, 94 (2015).

[11] G. Mourou, T. Tajima, Summary of the IZEST science and aspiration, *Eur. Phys. J. Spec. Top.* **223**, 979-984 (2014).

[12] T. Tajima, Laser acceleration in novel media, *Eur. Phys. J. Spec. Top.* **223**, 1037 (2014).

[13] V. Yakimenko, *et al.,* FACET-II facility for advanced accelerator experimental tests, *Physical Review Accelerators and Beams*, **22(10)**, 101301 (2019).

[14] S. Iijima, Helical microtubules of graphitic carbon, *Nature* **354**, 56 (1991).

[15] A. A. Sahai, T. Tajima, P. Taborek, and V. Shiltsev, Solid-state tube accelerator using surface wave wakefields in crystals, in *Beam Acceleration in Crystals and Nanostructures*, Eds. S. Chattopadhay, G. Mourou, V. Shiltsev, T. Tajima (World Scientific, Singapore, 2020) p.123.

[16] S. Hakimi, T. Nguyen, C.K. Lau, D. Farinella, H. Wang, P. Taborek, and T. Tajima, Wakefield simulation of solid state plasma, *Phys. Plas.* **25**, 023112 (2018).

[17] T. Tajima, S. Ushioda, Surface polaritons in LO-phonon-plasmon coupled systems in semiconductors, *Phys. Rev. B* **18**, 1892 (1978).

[18] P. San Miguel Claveria *et al.*, Spatiotemporal dynamics of ultrarelativistic beam-plasma instabilities, arXiv:2106.11625 (2021).

[19] E. Lefebvre *et al.*, Electron and photon production from relativistic laser plasma interactions, *Nucl. Fusion* **43**, 629 (2003).

[20] A. Benedetti, M. Tamburini and C. H. Keitel, Giant collimated gamma-ray flashes, *Nat. Photon.* **12**, 319 (2018).

[21] B. Hidding *et al.*, Ultracold Electron Bunch Generation via Plasma Photocathode Emission and Acceleration in a Beam-Driven Plasma Blowout, *Phys. Rev. Lett.* **108**, 035001 (2012).

[22] E. Adli *et al.*, Acceleration of electrons in the plasma wakefield of a proton bunch, *Nature* **561**, 363 (2018).

[23] M. Turner *et al.*, Experimental Observation of Plasma Wakefield Growth Driven by the Seeded Self-Modulation of a Proton Bunch, *Phys. Rev. Lett.* **122**, 054801 (2019).

[24] V. Yakimenko *et al.*, Prospect of Studying Nonperturbative QED with Beam-Beam Collisions, *Phys. Rev. Lett.* **122**, 190404 (2019).

[25] A. Sampath *et al.*, Extremely Dense Gamma-Ray Pulses in Electron Beam-Multifoil Collisions, *Phys. Rev. Lett.* **126**, 064801 (2021).

[26] B. S. Nicks, T. Tajima, D. Roa, A. Necas, and G. Mourou, Laser-wakefield application to oncology, *Int. J. Mod. Phys. A* **34**, 1943016 (2019).

[27] D. Roa, *et al.*, Rationale for using a C-arm fluoroscope to deliver a kiloVoltage radiotherapy treatment to COVID-19 patients, *Med. Dos.* **46**, 1(2021) Letter (DOI:https://doi.org/10.1016/j.meddos.2020.07.008)

[28] D. Roa, *et al.*, Monte Carlo simulations and phantom validation of low-dose radiotherapy to the lungs for an interventional radiology C-arm fluoroscope, *Physica Medica* **94**, 24 (2022).

[29] K. Matsumoto, *et al.*, Destruction of tumor mass by gadolinium-loaded nanoparticles irradiated with monoenergetic X-rays: implications for the Auger therapy, em Sci. Rep. **9**, 13275 (2019).

[30] V. Shiltsev, On possibility of low emittance high energy muon source based on plasma wakefield acceleration, FNAL-Pub-2022-137 (submitted to *JINST*, 2022)